Electromechanical Milling - Conception and Design of the Excitation System

B. Halbedel

Technische Universität Ilmenau, Institute of Materials Engineering,
Department of Inorganic-Nonmetallic Materials, Group of Materials research in or with Magnetic Fields
Gustav-Kirchhoff-Straße 6, D-98693 Ilmenau, Germany

Corresponding author: bernd.halbedel@tu-ilmenau.de.

Abstract
The novel electromechanical milling principle is a solution providing reduced energy consumption with milling beads directly moved with a time- and local-variable magnetic field, which is generated in a working chamber by an external, electrical excitation system. Hence, the main design parameters of such machines for electromechanical milling (so-called EMZ plants) must be derived from the time- and local-variable magnetic flux density, the resulting vector gradient and the electromagnetic force distribution in the process room. For the calculation and optimization of these distributions we developed a numerical model on the basis of the commercial software tool ANSYS Maxwell®. We verified this model with experimental measurements of the electromagnetic field in the process room. Furthermore, we have studied the influence of the excitation system design on the vector gradient distribution and discuss selected results in this paper. The study identifies potentials for the further improvement of electromechanical units built in the past.

Key words: milling, electromagnetic field, simulation, optimization, design

1 Introduction

Milling is an important but very complicated and energy consuming process step in numerous material productions such as the preparation of raw or starting materials for the glass, ceramic and the building industry as well as the recycling of waste materials. State of the art is the mechanical grinding with different type of mills. Most used mills are ball mills e.g. in the field of cements production with an input power of up to 28 MW with pull rates of up to 350 t/h, lengths of up to 15 m and diameters of up to 12,8 m [1]. However, the energy efficiency of such mills is disastrous, e.g. the energy efficiency of ball mills is < 9 % or of jet mills even < 2 % [2]. Thus, about 91 % up to 98 % of the input power are losses. These large power parts do not contribute to particle size reduction and are wasted. Therefore, the energy efficiency improvement of the milling machines is an important goal of current research and development activities and a necessary component of environmental strategies [3-6]. The low energy efficiency is caused by the indirect motion of the milling beads connected with high energy losses. Therefore, pivotal questions for the improvement of a novel mill conception are:

+ Can we move the milling beads directly, e.g. with magnet fields?
+ Is the movement of the milling beads enough intense and relative together?

The last requirement is important for the generation of mechanical stresses at the material to be milled in the process room.
In *Section 2* the basics for electromagnetic movement of milling beads and the conception as well as the necessary base design of electromechanical mills as a result of the deduced conditions are explained. In *Section 3* an electromagnetic model based on the commercially available software tool ANSYS Maxwell® for the design of the excitation system – the most important component of electromechanical milling machines – is introduced. *Section 4* presents the simulated vector gradient distributions in the process room and how they are influenced by the design of the excitation system.
Finally, *Section 5* summarizes the main findings and ends with a perspective on further development of the electromechanical milling system.

2 The electromechanical milling principle (EMZ)

2.1 Basics

A milling bead moves in a magnetic field if

a) the milling bead is hard magnetic, i.e. milling beads have a fixed magnetization and
b) the magnet field is nonhomogeneous, i.e. magnetic field exhibits a vector gradient

then an electromagnetic force $\vec{F}_{\nabla\vec{B}}$ on a milling bead is generated as shown in Fig. 1. The generated force of one milling bead is given by equation (1) and (2):

$$\vec{F}_{\nabla\vec{B}} = (\vec{p}_M \cdot \nabla)\vec{B}\,, \tag{1}$$

where $\vec{p}_M$ is the vector of the magnetic moment, given for milling beads by

$$\vec{p}_M = \int_V \vec{M} dV = \frac{1}{\mu_0} \int_V \vec{J} dV \,, \tag{2}$$

with $\vec{M}$ – the fixed permanent magnetization of the milling beads, $\vec{J}$ – its magnetic polarization, V – the volume of a milling bead and $\mu_0 = 4\pi \cdot 10^{-7}$ Vs/Am – the absolute permeability.

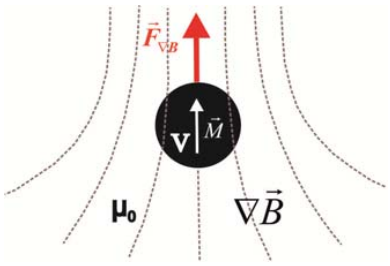

Fig. 1. Magnetic force $\vec{F}_{\nabla\vec{B}}$ on a milling bead with a magnetization $\vec{M}$ and the volume V in a magnetic field $\vec{B}$ with a vector gradient $\nabla\vec{B}$

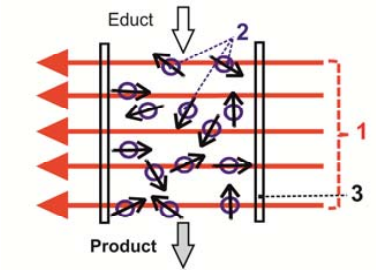

Fig. 2. Conception of an electromechanical mill (EMZ)
1 - time- and local-variable magnet field, 2 - hard magnetic milling beads, 3 - process room

With the simplifying assumptions that the magnetization of the milling bead is $\vec{M} = M = const.$ in its volume and directed in the same direction as $\nabla\vec{B}$ we can deduce equation (3) for description of the electromagnetic force density $\vec{f}_{\nabla\vec{B}}$ on one milling bead:

$$\vec{f}_{\nabla\vec{B}} = \frac{\vec{F}_{\nabla\vec{B}}}{V} = M \cdot (\nabla\vec{B}) = \frac{1}{\mu_0} J \cdot (\nabla\vec{B}) \,, \tag{3}$$

with M – magnitude of the magnetization $\vec{M}$ and J – magnitude of magnetic polarization $\vec{J}$.

As revealed in equation (3) the vector gradient of the magnetic field $\nabla\vec{B}$ dictates the direction of the force density $\vec{f}_{\nabla\vec{B}}$ and the product $J \cdot (\nabla\vec{B})$ determines its magnitude.

Additionally, if the magnetic vector gradient is time- and local-dependent, then a time- and local-dependent force density distribution $\vec{f}_{\nabla\vec{B}(r,\varphi,z,t)}$ is generated in the process room, consequently intensive relative movements between several milling beads are induced with different types of mechanical stresses so that the novel electromechanical milling principle can be used for disintegration of biomass, dry or wet grinding of raw materials and autogenous grinding of ferrites [7, 8].

2.2 Base Design

For the technical implementation of such requirements it is necessary to build a process room (cf. Fig. 2) – the best layout is an annular gap - with non-ferromagnetic walls, which is

+ penetrated from a time and local variable electromagnetic field $\vec{B}$ - generated from a multi-phase electrical exciter system surrounding the process room and
+ filled with numerous and freely movable hard magnetic milling beads.

Then the magnetic field in the process room is nonhomogeneous and exhibits a time and local variable vector gradient distribution, which generates a time and local variable force distribution on the milling beads, whereof

+ intensive relative motions of the milling beads in the process room result and
+ different types of mechanical stresses on powders or in suspensions develop (e.g. friction, shear, impact) which different types of preparation effects of powders or in suspensions generate (e.g. deagglomeration, disintegration, dispersion, grinding).

All these are mainly dependent on the design of the excitation system and its operating parameter. Therefore, we need a model for the determination of the optimal design and for adaption of the operating parameter of the EMZ machine.

3. Model for electromagnetic design

Our developed electromagnetic model for the design of the exciter system of the EMZ machine is based on the following important steps:

1) Simulation of the magnet flux density distribution $\vec{B}(r,\varphi,z,t)$ in the draft of the exciter system of the EMZ machine,

2) Determination of the vector gradient distribution $\nabla\vec{B}(r,\varphi,z,t)$ in the process room dependent on design parameters (e.g. width of the process room, type of winding, number of poles and of phases) as well as on operating parameters (e.g. mean magnetic field strength, phase number, frequency of electric current) and
3) Selection of the design and operating parameter with the adequate vector gradient distribution in the process room.

The simulation of the magnetic field distribution $\vec{B}(r,\varphi,z,t)$ in the exciter system is carried out in ANSYS Maxwell® by iterative solution of the partial differential equations (4) and (5)

$$\nabla\times(\frac{1}{\mu}\nabla\times\vec{A})=\vec{j} \qquad \text{and} \qquad \vec{B}=\nabla\times\vec{A} \qquad \text{(4) and (5)}$$

with $\vec{A}$ as the magnetic vector potential resulting from the design of the windings and the electric current distribution $\vec{j}$ in the exciter system and with μ as the magnetic permeability in the solution domains.

For the determination and evaluation of the vector gradient distribution in the process room, we must discretize the process room again, in 2D only (see Fig. 3) because the z component of the magnet flux density is negligibly small.

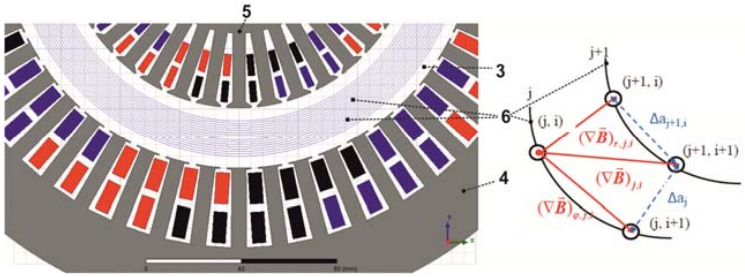

Fig. 3. Extract from a 2D model of an excitation system (*left*) with the details of the discretization of the process room for the calculation of the magnet vector gradient components $(\nabla B)_{r,j,i}$ and $(\nabla B)_{\varphi,j,i}$ in the points (*i, j*) (*right*)
3 - process room, 4 - outer part and 5 -inner part of the excitation system, 6 – *j* circles with the radii R_j and distance Δa_j

Taking wall thickness of the process chamber and sizes of the used milling beads into account, we define *j* circles with radii R_j and n_j points with the distances Δa_j and $\Delta a_{j,i}$. Then we calculate the *r* and φ components of the vector gradient $(\nabla\vec{B})_{j,i}$ in each point *(j, i)* on the base of the simulated magnetic flux density distribution $\nabla\vec{B}(r,\varphi)$ to a fixed time, e.g. $\omega t = 0$, with the equations (6):

$$(\nabla\vec{B})_{j,i}=(\nabla B)_{r,j,i}\cdot\vec{e}_r+(\nabla B)_{\varphi,j,i}\cdot\vec{e}_\varphi=(\frac{\partial B_{r,j,i}}{\partial r}+\frac{1}{r_j}\frac{\partial B_{r,j,i}}{\partial\varphi}-\frac{B_{\varphi,j,i}}{r_j})\vec{e}_r+(\frac{\partial B_{\varphi,j,i}}{\partial r}+\frac{1}{r_j}\frac{\partial B_{\varphi,j,i}}{\partial\varphi}+\frac{B_{r,j,i}}{r_j})\vec{e}_\varphi \qquad (6)$$

For the evaluation of different design layouts as well as operating parameter we use the RMS value of the vector gradient components of selected circles *j* with equation (7) and (8).

$$(\nabla B)_{r,j,eff}=\sqrt{\frac{1}{n_j}\cdot\sum_{i=1}^{j}((\nabla B)_{r,j,i})^2} \quad \text{and} \qquad (\nabla B)_{\varphi,j,eff}=\sqrt{\frac{1}{n_j}\cdot\sum_{i=1}^{j}((\nabla B)_{\varphi,j,i})^2} \qquad \text{(7) and (8)}$$

with n_j as the number of points *(j, i)* on the circle *j*.

The electromagnetic model was evaluated with experimental measurements of the magnetic flux densities in the process room and comparison simulations in COMSOL Multiphysics [7, 9].

4. Results and discussion

Fig. 4 presents the simulated vector gradient distributions of the radial and azimuthal component in the process room of an electromechanical lab mill on three selected circles, which are located in the near of the inner part of the excitation system (R1), in the middle of the process room (R8) and close to the outer part (R16) of the excitation system at a mean magnetic field strength of H_δ = 70 kA/m and a frequency of f = 50 Hz.

The components of the vector gradient of the magnetic field have the same order of up to about 10 T/m, but their changes are larger close to the exciter systems (circle R1 and R16) than in the center (circle R8) of the process room. Consequently, the milling beads are more accelerated or decelerated close to the excitation system. Here the movement changes are maximal.

In the center of the process room the distributions are approximately sinusoidal along the circle R8. However, they are shifted, so that the azimuthal component $(\nabla B)_{\varphi,j}$ is larger where the radial component $(\nabla B)_{r,j}$ is smaller or vice versa.

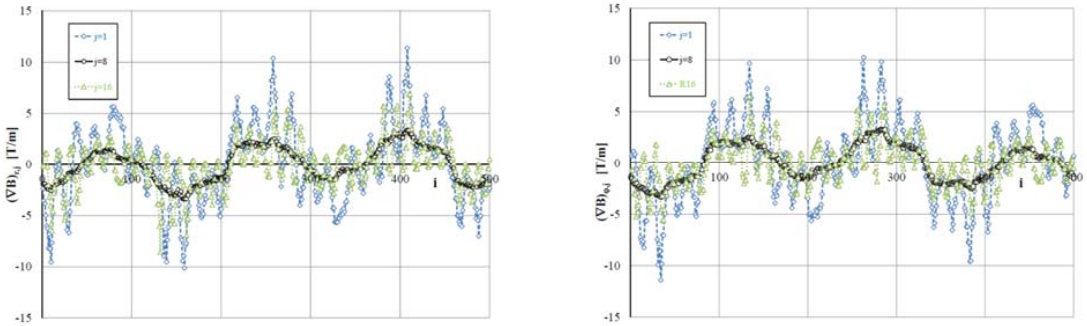

Fig. 4. Radial $(\nabla B)_{r,j}(i)$ (*left*) and azimuthal $(\nabla B)_{\varphi,j}(i)$ (*right*) components of the vector gradient of the magnetic field in the process room of a electromechanical lab mill on three circles j, which are located in the near inner part of the excitation system (R1), in the middle (R8) of the process room, and close to the outer part of the excitation system (R16) dependent on i at H_δ = 70 kA/m, f = 50 Hz, ωt = 0

Other simulations show that the RMS values of the vector gradient components increase with the enhancement of the mean magnetic field strength H_δ in the process room (see Fig. 5). The mean magnetic field strength H_δ in the process room results from the magnitude of electric currents in the coils and their layout.

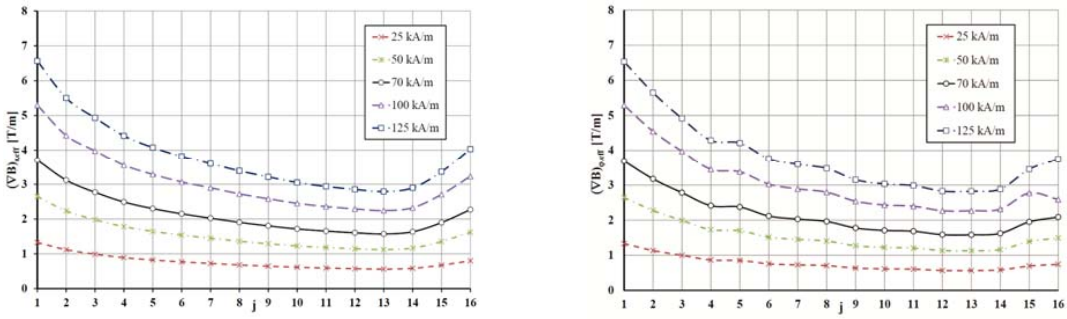

Fig. 5. Distributions of the RMS values of the radial $(\nabla B)_{r,eff}$ (*left*) and azimuthal $(\nabla B)_{\varphi,eff}$ (*right*) components of the vector gradient over the width of the process room dependent on the mean magnetic field strength H_δ for f = 50 Hz and ωt = 0

The graphs show that the RMS values of the vector gradient components on the circles j are about same. Hence, the milling beads are approx. uniformly distributed in the r - φ plane of the process room [7]. But, how we have seen in the diagrams in Fig. 4, the RMS values of the vector gradient components are larger close to the exciter systems than in the vicinity of the outer excitation system. This disparity increases with larger magnet field strengths in the process room. The reason is the realized ampere turns in the inner and outer parts of the excitation system.
Further crucial influencing factors on the vector gradient components are the windings layout and the number of poles. It is possible to perform the windings of the excitation system as distributed windings or as concentrated two-layer and single-layer windings. The simulations prove that concentrated windings generate larger vector gradients in the process room at the same operating parameters (see Fig. 6).

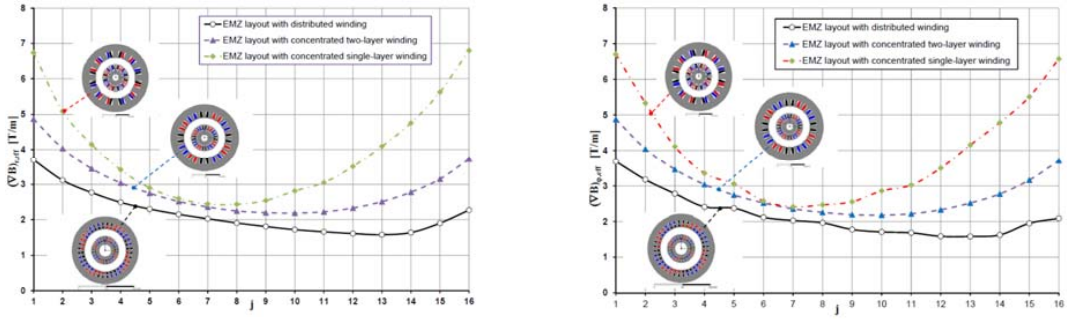

Fig. 6. RMS value distribution of the radial $(\nabla B)_{r,eff}$ (*left*) and azimuthal $(\nabla B)_{\varphi,eff}$ (*right*) components of the vector gradient in the process room for different windings layouts of the excitation system at H_δ = 70 kA/m, f = 50 Hz, ωt = 0

When the magnetic vector gradient is larger, the milling beads move more intensively und the mill produces a finer product at the same operating parameters. Moreover, the heights of its end turns are smaller and consequently there is less cupper required for the fabrication of the windings. This is an important additional advantage for design of EMZ devices [10].
Also the adjustment of number of poles $2p$ dependent on the dimension of the electromechanical mill as well as the reduction of the number of slots per pole per phase q and of the chording of the windings ε are potentials for further improvements of the performance of mills based on the electromechanical principle [10].

5. Summary and Outlook

The theoretical investigation of the function of the novel electromechanical milling principle and the study of the design of the excitation system – the most important component of electromechanical milling machines – together with the developed electromagnetic model based on the commercially available software tool ANSYS Maxwell® show that the distribution of the magnetic vector gradient in the process room of electromechanical mills determine the movement of the milling beads and thereby also the milling result [7, 8]. The study of the influence of the excitation system design on the vector gradient distribution identifies potentials for the further improvement of electromechanical lab units built in the past [12, 13]. In particular, the design of the windings of the excitation system provides great potential for further improvement. The next steps are the connection of developed electromagnetic model with DEM-simulations [14] and a stress model [15] to determine the required magnet field structure in the air gap for an efficient milling process.

Acknowledgment
The authors acknowledge financial support by the German Research Foundation (DFG) (Ha 2338/1) and by the Federal Ministry for Economic Affairs and Energy (BMWi) in ZIM-Cooperation Project EMZ-W (KF2184744KO4) as well as support by several industrial partners and former co-workers for their major commitment.

References

1. http://www.at-minerals.com/de/artikel/at_2010-10_Groesste_Muehle_der_Welt_1003987.html (23.05.2018)
2. Pahl, M. H.: Zerkleinerungstechnik. 2. Auflage, Fachbuchverlag Leipzig/Verlag TÜV Rheinland, 1993.
3. Schäfer, St. and Hoenig, V.: Chancen und Grenzen der energetischen Optimierung und CO_2-Reduktion in der Zementindustrie. 2. Energiepanel Energieeffizienz und CO_2-Reduktion in der Industrie Mainz, 25.03.2015.
4. Shi, F., Morrison, R, Cervellin, A., Burns, F., Musa, F.: Comparison of energy efficiency between ball mills and stirred mills in coarse grinding. Minerals Engineering, Volume 22, Issues 7–8, pp 673-680, June–July 2009.
5. Schubert, G.: How to Make Milling More Energy Efficient. PROCESS Worldwide, Volume 13, No. 3, pp 19-21, June 2011.
6. Bakker, J.: Energy Use of Fine Grinding in Mineral Processing. METALLURGICAL AND MATERIALS TRANSACTIONS E, Vol. 1E, pp 9-19, March 2014, DOI: 10.1007/s40553-013-0001-6.
7. Halbedel, B., Kazak, O.: Potenziale eines neuen Mahlverfahrens – Die elektromechanische Zerkleinerung (EMZ) (Potential of a New Milling Principle – The Electromechanical Milling). Chem.-Ing. Tech., Vol. 90, Issue 4, pp 540-551, April 2018, DOI: 10.1002/cite.201700103.
8. Halbedel, B., Kazak, O.: Development of electromechanical principle for wet and dry milling. IOP Conf. Ser.: Mater. Sci. Eng. 355 012021, 8 pages, 2018, DOI 10.1088/1757-899X/355/1/012021.
9. Kazak, O.; Halbedel, B.: Approaches for modelling electromagnetic parameters in milling demonstration plant of organic agents. In: Proceedings 8th International Conference Electromagnetic Processing of Materials, Cannes/ France, 12 – 16 October, 2015.
10. Halbedel, B.; Kazak, O.: Vorrichtung und Verfahren zum Zerkleinern, Desagglomerieren, Dispergieren und Mischen von dispersen Stoffen und pumpfähigen Mehrphasengemischen. DE 10 2017 008 513.7, registered: 06.09.2017.
12. Halbedel, B.; Müller, W.; Baudrich, R.; Hülsenberg, D.: Process and apparatus for reducing, dispersing, wetting and mixing pumpable, non-magnetic multiphase mixtures. US 5,348,237, 19.12.1991.
13. Halbedel, B.; Hülsenberg, D.: Elektromechanische Zerkleinerung. In: Technische Keramische Werkstoffe, John von Freyend GmbH, Fachverlag für Wirtschaft und Außenhandel, Köln, Nov. 1995.
14. https://www.cfdem.com/liggghts-open-source-discrete-element-method-particle-simulation-code, 28.05.2018
15. Kwade, A.: A Stressing Model for the Description and Optimization of Grinding Processes. Chemical Engineering & Technology 26 (2) 199 – 205, 2003, DOI: 10.1002/ceat.200390029.